Werk

Jahr: 1987
Kollektion: fid.geo
Signatur: 8 Z NAT 2148:61
Digitalisiert: Niedersächsische Staats- und Universitätsbibliothek Göttingen
Werk Id: PPN1015067948_0061
PURL: http://resolver.sub.uni-goettingen.de/purl?PPN1015067948_0061

LOG Id: LOG_0028
LOG Titel: Systematics of arc-associated electric fields and currents as inferred from radar backscatter measurements
LOG Typ: article

Übergeordnetes Werk

Werk Id: PPN1015067948
PURL: http://resolver.sub.uni-goettingen.de/purl?PPN1015067948
OPAC: http://opac.sub.uni-goettingen.de/DB=1/PPN?PPN=1015067948

Contact

Niedersächsische Staats- und Universitätsbibliothek Göttingen
Georg-August-Universität Göttingen
Platz der Göttinger Sieben 1
37073 Göttingen
Germany
Email: gdz@sub.uni-goettingen.de

J Geophys (1987) 61:122–137

Journal of Geophysics

Systematics of arc-associated electric fields and currents as inferred from radar backscatter measurements

E.E. Timofeev[1], M.K. Vallinkoski[2], T.V. Kozelova[1], A.G. Yahnin[1], and R.J. Pellinen[2]

[1] Polar Geophysical Institute, Kola Branch of the USSR Academy of Sciences, 184200 Apatity, Murmansk region, USSR
[2] Finnish Meteorological Institute, Department of Geophysics, Box 503, SF-00101, Helsinki, Finland

Abstract. Observational data from all-sky cameras, ionosondes, riometers, ground-based magnetometers and from a 90 MHz short-pulse auroral radar have been used in the analysis of 41 auroral arc events in the interval 18-06 MLT over Scandinavia and the Kola peninsula during the IMS period. The spatial distributions of electric fields in the vicinity of the auroral arcs were determined by radar data, which were sometimes supplemented by balloon and rocket data. The study leads to the following conclusions: (*i*) At ionospheric level, the arc-associated electric field has a meridional scale of about 1° in latitude for all MLT values. This is equally true for active and quiet auroral arcs. (*ii*) Far from midnight, the spatial orientation of the field closely follows the orientation of the ionospheric convection electric field. The maximum of the arc-associated electric field is observed equatorward of the visual arc in the evening and poleward in the morning. (*iii*) Near midnight, after the convection reversal, the behaviour of the arc-associated electric field on the southern edge of the auroral bulge is of the evening type, while at the northern edge of the bulge it is of the morning type. In the evening type, the meridional component of the ambient electric field vanishes, while the morning type is characterized by the dominance of the southward component of the electric field. Radar diagnostics show that the minimum meridional distance between the visual arc and the radar arc is, on average, about zero in the evening and about 15 km in the morning. (*iv*) The work done by the arc-associated electric field within the radar arc but outside the visual arc is positive in all MLT sectors, and it is concluded that the generator of the arc-associated electric field is located in the magnetosphere. By using possible conductivity profiles through the arc, models of the three-dimensional current system associated with an auroral and radar arc are built. These results are compared with direct measurements and discussed in the light of the main models of the electrodynamical structure of auroral arcs.

Key words: Ionosphere – Radar aurora – Electric field – Auroral arc – Convection – Conductivity profiles – Three-dimensional currents – Arc-associated electric field

Introduction

An optical auroral arc, quiet or disturbed, has a large number of couplings to the surrounding ionosphere, to the magnetosphere and even to the interplanetary medium. The electric field measured in the vicinity of an auroral arc is a superposition of the large-scale, convective magnetospheric electric field, obviously controlled by the interplanetary electric and magnetic fields (Akasofu, 1981), the electric field associated with the inverted-V containing the arc (Heelis et al., 1981; Timofeev et al., 1985a), and the local electric field produced by the arc itself (Marklund et al., 1982; Ziesolleck et al., 1983). The convective electric field in the auroral oval region is typically of the order of some mV/m, while the electric field produced by the inverted-V and the auroral arc may vary from a few tens to 100 mV/m (Heelis et al., 1981; Timofeev et al., 1983, 1985a). The region directly influenced by the auroral arc and inverted-V electric fields has a meridional scale varying from 10 to 100 km. Inside the arc itself, there is a distinct structure with a meridional scale of 10 km (Marklund et al., 1982). In this paper we shall call the electric field produced by the arc itself, superimposed on the inverted-V electric field and observed locally in the vicinity of the arc, 'the arc-associated electric field'.

The electric fields observed in the auroral arc region depend strongly on the current systems coupling the auroral oval to the outer magnetosphere. An observed electric field is a superposition of the two electric fields mentioned above. In order to discuss the arc-associated electric field one has to be able to subtract the convective field from the observed total electric field. This may be difficult in practice, especially during disturbed conditions, since both the convective electric field and the field-aligned Birkeland currents influence the arc environment.

During the past few years, numerous measurements of electric fields, conductivities and currents in the vicinity of an auroral arc have been made by means of rockets, satellites and incoherent scatter radar facilities [e.g. see Baumjohann (1983) and Marklund (1984) and references therein]. A rather complete set of such data in the evening sector has made it possible to study different types of electric field patterns near an auroral arc (de la Beaujardière et al., 1981). On the other hand, similar data in the morning sector are scanty. There are (up to 1985) only four cases of direct measurements: de la Beaujardière et al. (1977), Horwitz et al. (1978), Ziesolleck et al. (1983) and Brüning et al. (1985). It is worthwhile to note that in the first two cases the auroral forms studied were homogeneous long-lived arcs, and the latitudinal scan of the incoherent scatter radar used was of the order of 10 min or more; while in

the last two cases rocket data were used and the arcs were somewhat active. The study of the parameters of an active arc, observed as a rule in the near-midnight sector of magnetic local time (MLT), is difficult because of the dynamical nature of the arc. Therefore, the data on electric fields and currents around such arcs are actually non-existent except for the events described on the basis of STARE data (STARE = Scandinavian Twin Auroral Radar Experiment, Greenwald et al., 1978; Nielsen and Greenwald, 1978; Inhester et al., 1981; Baumjohann et al., 1981). However, in these cases it is difficult to distinguish an arc-associated electric field from the large-scale convection electric field or bulge-associated electric field because the STARE radial resolution is only about 15 km, whereas the spatial scale of the arc-associated field is of the order of 10 km (Marklund et al., 1982; Ziesolleck et al., 1983). The rocket data on electric field patterns associated with an individual active auroral arc have rather insufficient coverage because of the strong temporal and spatial dynamics of the visual arcs during the flight.

The first study on radar arcs (Chesnut, 1968) was made about the radiophysical characteristics of the phenomenon. Tsunoda et al. (1976) were the first to draw conclusions about the spatial structure of the electric fields and currents in the vicinity of an auroral arc. However, these results were limited to the evening sector, and the spatial resolution was 45 km.

This paper aims at a systematic investigation of the configurations of electric fields and currents around an auroral arc in different MLT sectors and under varying ionospheric conditions. For this purpose, we have used PPI (Plane Position Intensity) data of a rotating radar antenna on discrete radar arcs, along with data from ionospheric and ground-based measurements. The pulse length of 8 μs gives a slant range cell length of only 2 km in the direction along the radar beam. In practice, this means that the radial resolution is about 5 km. Since the beam width was 9°, the lateral resolution is much poorer: of the order of 100 km in practice. The radar is about 15 dB less sensitive than STARE, so that the results presented here cannot be directly compared with STARE data.

It is known that a rough linear dependence has been found between the radar aurora (RA) intensity and the ambient ionospheric electric field from threshold to about 30 mV/m (Tsunoda and Presnell, 1976; Siren et al., 1977; André, 1983), after which this dependence disappears (André, 1983; Uspensky et al., 1983). For electric fields well above the threshold, the radar aurora intensity has been found to be controlled by the ionospheric electron density only (Starkov et al., 1983). By using ionosonde, riometer chain and X-ray balloon data, we have checked whether the area of maximum electron density outside the auroral arc itself coincides with the location of the RA maximum intensity. This allows us to decide which parameter can be diagnosed by radar data *in situ*: electric field or electron density. Thus, for example, the appearance of a radar arc in a previously quiescent ionosphere, where the ambient electric field is evidently below the threshold, must be due to an increase in the electric field strength near the visual arc. Then, using simultaneous data from ground-based magnetometers, the sign of the meridional component of the ionospheric electric field can be inferred from the direction of the ionospheric Hall currents. Similar methods have been tested earlier by Timofeev et al. (1980) in studying the near-arc structure of the ionospheric currents in the evening sector. The conclusions obtained there are supported by direct measurements (Burke et al., 1980; Vondrak, 1981; Marklund et al., 1982; Baumjohann, 1983).

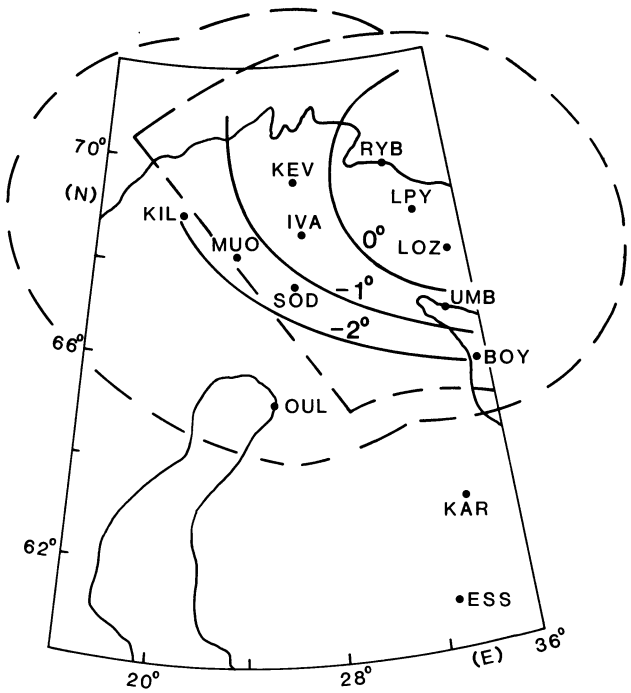

Fig. 1. The map of the observation region including the main Scandinavian and Kola peninsula observatories used. The general field of view of the ASCs limited by a zenith angle of 75° is shown by the *outermost dashed curve*. *Solid curves* are the aspect angle contours of the Essoyla radar, and the *innermost dashed curves* show the radar field of view

Table 1. The Essoyla radar parameters

Transmitter peak power	75 kW
Transmitter frequency	88 ± 5 MHz
Pulse width	8 μs
Horizontal beam width	9°
Antenna rotation period	72 s
Pulse repetition frequency	50 Hz

Experimental arrangements and data handling

The main part of the visual aurora data was obtained by the Finnish all-sky camera (ASC) network [for a description, see Pellinen (1982)], supplemented by ASC pictures from Loparskaya and Apatity, Kola peninsula. The positions of the main observatories are shown in Fig. 1. In addition, data from the Scandinavian Magnetometer Array (SMA), balloon and rocket measurements (e.g. SAMBO, SBARMO and Substorm-GEOS experiments) were used in several events. Observations of the radar aurorae were performed in the azimuth scan mode of the 90 MHz short-pulse radar located in Essoyla (61°N, 33°E), Karelia, USSR. The main technical parameters of the radar are given in Table 1.

The selected events with radar and visual auroral arcs and with direct ionospheric electric field measurements in the vicinity of a radar arc are from the period 1975–1982,

and mainly from midnight and morning sectors. Since the radar arc is, in general, more often associated with bright than with faint visual arcs, the selection is somewhat biased. The data set used consists of 15, 19 and 7 events in the morning, near-midnight and evening sectors, respectively. The well-studied evening sector part contains the cases of direct measurements or the most illustrative examples only. All events were selected to satisfy the following requirements:

1) the auroral arc is observed near the zenith of some ASC for at least 2 min

2) the meridional drift velocity of the arc does not exceed 200 m/s

3) the magnetometer data of the Kola peninsula chain from Rybatchy (RYB) to Umba (UMB) are available for this interval.

There are two exceptions to the first requirement. In these cases, the zenith angle was about 45°. For these two events, the projections of the lower edge of the arc on the map were estimated by first plotting the curves for the two extreme cases of arc altitudes, 90 and 120 km. The band between the two curves was then compared with the location of the corresponding radar arc. This procedure is the same as in the Radar – All-Sky Camera procedure (RASC) of Fremouw and Fang (1975).

In order to determine the minimum distances between the radar and visual arcs along the meridian, the morphological differences between evening and morning arcs have to be taken into account. Evening-type arcs are often relatively distinct with sharp boundaries, especially on the equatorward side, and relatively narrow in the latitudinal direction. The morning-type arcs are, on the other hand, wider and have more diffuse boundaries. Since the radar arcs appear equatorward of the evening arcs but poleward of the morning arcs, the minimum distance along the meridian is relatively easy to determine for evening arcs. For morning arcs, we selected out of the 19 cases available those 10 in which the auroral arcs were observed *constantly* in the zenith of some ASC, so that the distance determination was, in our opinion, as reliable as possible.

Observations and their interpretation

The evening sector

We shall present below two cases as illustrative examples of auroral arcs and associated magnetic variations, and two cases of direct measurements of the ionospheric parameters. We shall call the radar arcs appearing below 'evening radar arcs'.

Event 1. The ionospheric situation at 17.35 UT on March 3, 1976 is shown in Fig. 2. At that moment, the eastward electrojet suddenly intensified and reappeared for 1–2 min south of the Loparskaya station. The value of the *H*-component variation at the Lovozero station, under the southernmost auroral arc, was about 70 nT. It was a single arc accompanied by a radar arc located equatorward of the visual arc. It is to be noted that the radar arc was visible for 2 min, viz. the time of the electrojet recovery. The values of the *H*-component variations were negative north of Lovozero. One can also see that the bright auroral arcs embedded in the westward electrojet were not accompanied by radar arcs.

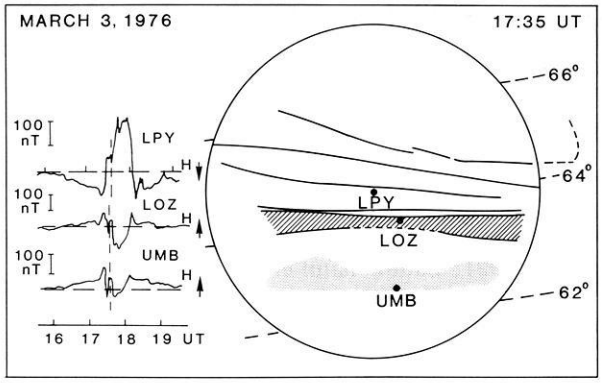

Fig. 2. Auroral arc and radar aurora display seen by the Loparskaya ASC (*solid circle*). Projections of auroral arcs are given by the *solid lines*. The radar arc is denoted by a *shaded band*. Diffuse luminosity is marked by *points*. The *dashed vertical line* on the Kola magnetometer chain (*left panel*) marks the moment of the radar arc appearance

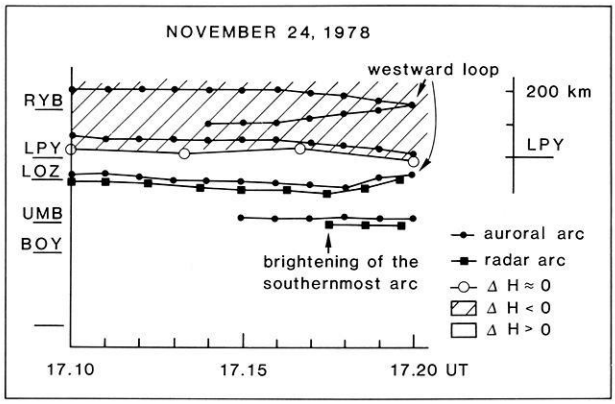

Fig. 3. The latitude-time diagram of the locations of auroral forms on November 24, 1978

Event 2. Figure 3 shows the latitudinal development of the electrojet boundary with radar and visual arcs between 17.10 and 17.20 UT on November 24, 1978. One can see that there were up to five auroral arcs within the latitudes from Rybatchy to Umba. The line $\Delta H = 0$, constructed from the data of the meridional magnetometer chain, divides the auroral arcs into two groups: those with and those without a radar arc. At first, only the southernmost auroral arc, embedded in the eastward electrojet, had a radar arc. Then at about 17.15 UT two auroral arcs appeared almost simultaneously, but on different sides of the boundary. Only the second southernmost auroral arc, located within the region of northward ambient electric field, was accompanied by a radar arc. According to the Kola peninsula magnetometer-chain data, the eastward electrojet intensified suddenly between 17.10 and 17.15 UT south of Loparskaya, within the region where the radar arcs appeared.

Event 3. March 5, 1979 is an example of balloon electric field measurements in the vicinity of an evening auroral arc during the SAMBO experiment. Figure 4 shows the electric field vectors measured by the three balloons plotted on the map. One can see a discrete auroral arc accompanied by a radar arc, situated near its equatorial edge. The electric field value decreased from 60 to 10 mV/m when passing

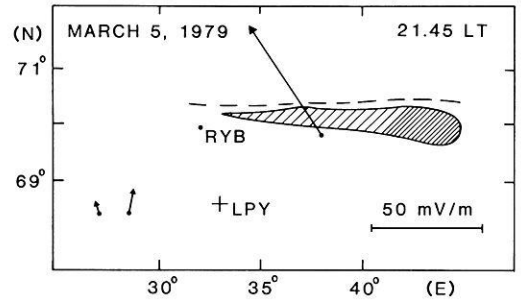

Fig. 4. The location of the aurora (*dashed line*) and the radar arc (*shaded band*) relative to the three SAMBO balloons. The *vectors* denote the electric field values measured by the balloons

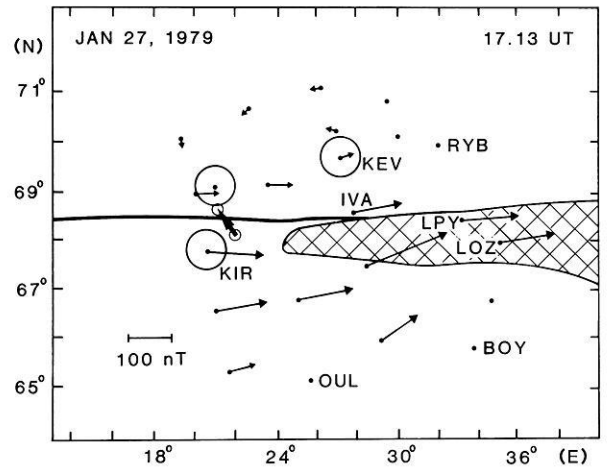

Fig. 5. The observation region during the GEOS-rocket launch. The *solid curve* shows the visual arc projection on the map according to the data from the three ASCs (*circles*), the *broad band* is the radar arc as seen by the Essoyla radar, and the *arrows* denote the ground equivalent current vectors. The projection of the rocket trajectory on the ionosphere is shown by the *thick arrow*

southward of the radar arc to a distance of about 1° in latitude. In agreement with the positive H-component variations registered by the ground magnetometers, the meridional component of the ionospheric electric field was directed northward according to all balloon data. The zonal, westward component of the electric field was negligible except in the vicinity of the auroral arc.

Event 4. January 27, 1979 gives an opportunity to study the behaviour of not only the electric field but also of other ionospheric parameters. The measurements were made by a rocket payload launched from Esrange at 17.12 UT during the Substorm-GEOS rocket experiment. The electron density and ionospheric current data, taken from Marklund et al. (1982), will be discussed later. The radar arc, appearing one-quarter of an hour earlier, was related to the brightening of the southernmost auroral arc. Both arcs are shown in Fig. 5 for the moment about 1 min after the launch. As is seen, a rather broad (up to 1° in latitude) radar arc was located close to the equatorial edge of the visual arc. Observations further to the west were impossible due to the large aspect-angle values. The rocket-borne electrometer registered the electric field north and east components with maxima of 115 and 20 mV/m, respectively, just before the equatorial edge of the visual arc. The measurements also showed the presence of a local electron density depression by a factor of 3–4 near the equatorial edge of the auroral arc [see Fig. 6 of Marklund et al. (1982)]. The maximum of the ionospheric current density was located at the southern edge of the auroral arc (Fig. 11a, ibid.). In other words, a current density enhancement was situated within the radar arc.

Therefore, the radar arc was a region of a Hall current located equatorward of the visual arc and propagating parallel with it, and the radar arc manifests itself in the evening sector as a westward Hall-current enhancement flowing at the equatorward side of the arc. The close spatial interrelation between the radar arc and the local electron density minimum mentioned is a typical feature of the evening arc. The same minimum can be clearly seen in Fig. 2.

However, sometimes, but rather rarely, the opposite occurs: the radar arc is situated right at the local ionization maximum. Two such exceptions have been observed in the evening sector, during growth phase conditions. The location of the moving ionization band was in these cases detected by riometer chain data. During the first event on November 11, 1976 the ionization band maximum observed at 17.06 UT near the Sodankylä zenith coincided with the centre of a broad radar arc with a thickness of some 20 km. During the second event on March 16, 1978 the absorption band passed the Loparskaya zenith at about 17.20 UT practically simultaneously with the passage of the radar arc. The absorption band location was determined in Starkov et al. (1980).

The morning sector (01–06 MLT)

In contrast to the evening, the appearance of a radar arc in the morning sector is connected with the increase in the westward electrojet intensity. Moreover, the radar arc shape is dissimilar to the regularly broadening shape of the evening radar arc, and it is observed on the poleward, opposite side of the visual arc. This spatial interrelation persists in this MLT sector independently of the location of other auroral forms (diffuse luminosity and absorption band) relative to the auroral arc. We shall illustrate this by describing three events, and we shall call the radar arcs appearing below 'morning radar arcs'.

Event 1. January 25, 1979. During this event, the auroral activation began in the region of the Kevo observatory at 01.50 UT (about 04.50 MLT). Before this time, the ionospheric currents had been quiescent for 3 h. Auroral arcs moved southward, brightening from time to time. One of these brightenings took place near the zenith of the Loparskaya observatory. Figure 6 shows the locations of the visual and radar arcs for this moment, as well as the magnetometer H-component record. As seen, the appearance of a radar arc poleward of the visual arc was accompanied by a sudden increase in the westward electrojet intensity. Diffuse, but remarkably intense luminosity was observed at the same side of the visual arc. The intensity of the backscattered signal had a maximum at the western edge of the radar arc and decreased in a regular manner towards the east along the arc. The Murmansk ionosonde registered a particle E-layer (E_{sr}) equatorward of the visual arc at 05.05 MLT, and r- and a-types of auroral ionization simultaneously poleward of the arc at 05.15 MLT. The electron densities determined for both moments from the f_B values

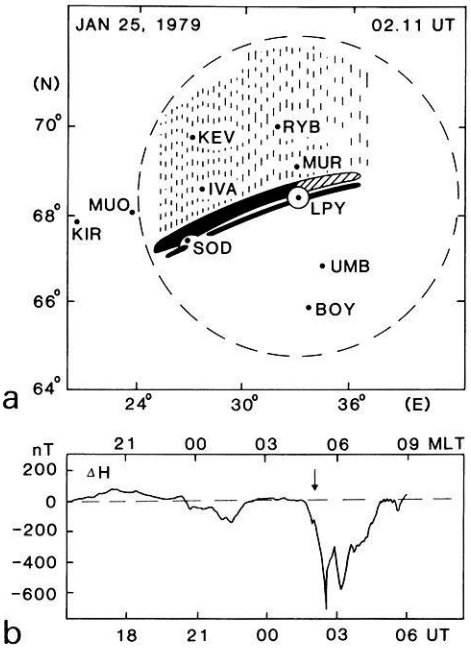

Fig. 6a and b. **a** Positions of the visual arc (*solid curve*) and of the radar arc (*broad band*). The *dashed region* is the region of diffuse luminosity. The *dashed circle* shows the field of view of the Loparskaya ASC. **b** The moment of interest on the Loparskaya magnetometer record is shown by an *arrow*

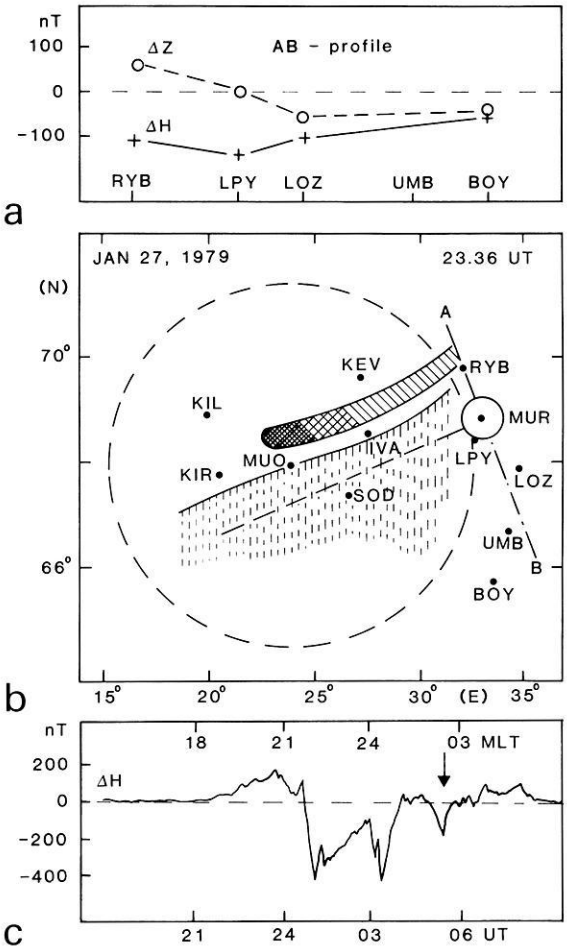

Fig. 7a–c. **a** Latitudinal profiles of the *H*- and *Z*-component variations at the moment of the auroral arc brightening. **b** The auroral arc (*solid line*) and radar arc (*broad band*) within the Muonio ASC field of view (*large dashed circle*) for the same moment. The intensity level of the radar arc is shown by the degree of darkening in the broad band. The *dashed region* is the region of diffuse luminosity. The *dashed straight line* shows the location of the centre of the auroral absorption band. The *solid circle* represents the ionosonde antenna beam cross-section. **c** The *arrow* on the panel marks the moment of interest in the Loparskaya magnetometer record

for the particle E-layer were approximately the same, about 2.2×10^{11} m^{-3}. The Loparskaya 32 MHz riometer directed to the North Star registered increased auroral absorption beginning at 04.45 MLT (01.45 UT). The maximum value of absorption, about 0.6 dB, was observed at 05.07 MLT when the riometer antenna beam pointed equatorward of the visual arc.

The ionization value registered during the event was well above the threshold of radar aurora appearance, which is equal to 3×10^{10}–5×10^{10} m^{-3} (Tsunoda and Presnell, 1976). Therefore, the absence of a radar aurora everywhere in the ionosphere, except in the narrow band poleward of the visual arc, means that the background electric field was less than the threshold electric field value. In our opinion, the *total* ionospheric electric field (background plus arc-associated) within the radar arc limits was already above the same threshold. Inferring from the sign of the *H*-component variation, both electric fields had southward meridional components.

Event 2. January 27, 1979. The riometer data of the event give an opportunity to detect accurately the meridional location of the auroral absorption band relative to the radar and visual arcs. The equatorward drift of the band and both arcs began at 02.19 MLT with an average velocity of about 200 m/s. The absorption maximum was registered at the Kevo and Ivalo observatories about 10 min before the radar arc crossed the zenith. Hence, the band maximum should be located about 120 km south of the centre of the radar arc at that time. According to the Murmansk ionosonde data ($f_B E_s$), the E-region ionization level in the event was 1.8×10^{11} m^{-3} at 02.15 MLT, and 1.4×10^{11} m^{-3} at 02.45 MLT. At 02.30 the ionosonde registered a blackout. Thus, during the whole time interval around the moments shown in Fig. 7, the ionization value was well above the threshold within the region equatorward of the visual arc. The backscatter signal intensity poleward of the arc increased suddenly at 23.36 UT (02.36 MLT) simultaneously with the brightening of the auroral arc. As seen from the magnetogram in the lower panel, the intensity of the ionospheric currents was nearly maximum at that moment. The profiles of the *H*- and *Z*-component variations constructed almost along the geomagnetic meridian are shown in Fig. 7a. One can see that the local maximum of the westward ionospheric Hall currents was located near the Loparskaya observatory, south of the visual arc. The radar arc was situated on the poleward side of the visual arc, and the backscatter intensity had a maximum at the western edge of the radar arc as in the previous event.

Hence, we can conclude that the riometer absorption and the energetic (20–30 keV) electron precipitation had a maximum equatorward of the arc. Since the ionization level was well above the threshold in this region, the pres-

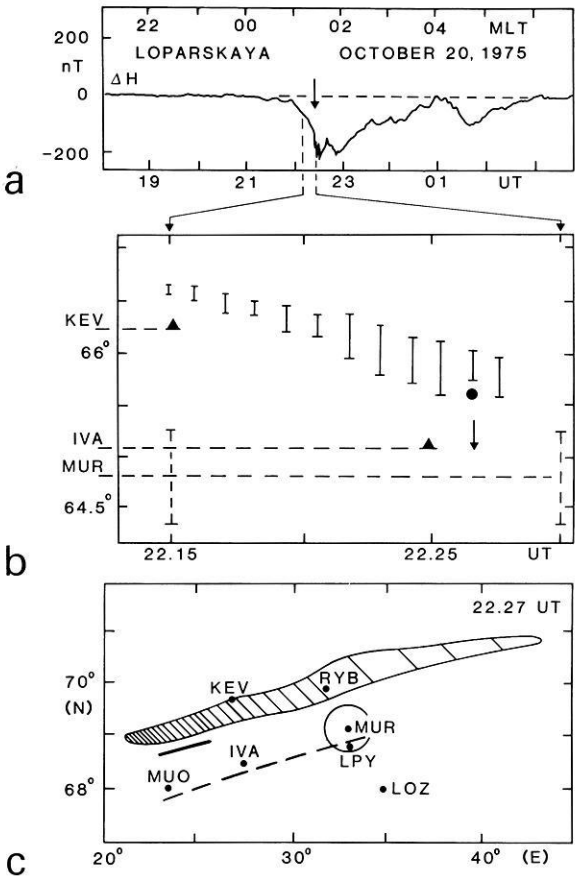

Fig. 8a–c. **a** The Loparskaya magnetometer record. **b** The corrected geomagnetic latitudes of the auroral forms versus UT of the riometer absorption band (*triangles*), the radar arc (*vertical segments*) and the visual arc (*solid circle*). *Dashed straight vertical segments* show the latitudinal size and location of the Murmansk ionosonde antenna beam cross-section. **c** Locations of all auroral forms at the moment of the arc brightening. The radar arc, visual arc and the riometer absorption band position are denoted by the *broad band, solid thick line* and the *dashed line*, respectively

ence of a backscatter band at the opposite side of the visual arc means that the ionospheric electric field there was strong and above threshold. Altogether, this means that the arc-associated electric field was southward and had a maximum within the radar arc, poleward of the visual arc.

Event 3. October 20, 1975. A weak, scattered arc was observed during the growth phase of an isolated substorm from 22.15 until 22.25 UT (01.15–01.25 MLT). The pre-substorm conditions can be clearly seen after 22.00 UT in the Loparskaya magnetometer data shown in Fig. 8a. This is in complete agreement with the IMP-8 satellite data (not shown here), according to which B_z (the z-component of the interplanetary magnetic field in the GSM-coordinate system) was positive (northward) for about 1 h before 22 UT and became negative right after that moment. The radar arc and the auroral absorption band drifted equatorward during the time interval considered here. The location of the absorption band was detected by the riometers at Kevo, Ivalo, Sodankylä and Loparskaya observatories. Before 22.27 UT, no aurora could be registered since the weather was cloudy. At 22.27 UT, an auroral arc poleward of the Muonio station brightened simultaneously with a

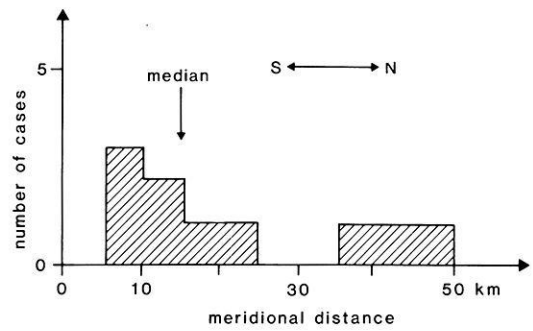

Fig. 9. The distribution of the minimum meridional distances between the radar and visual arcs in the morning. The median is marked by the *arrow*

sudden increase of the radar arc backscatter intensity. As seen in the magnetogram in Fig. 8a, the intensity of the ionospheric currents increased at the same moment, marked by the arrow. The locations of the radar and visual arcs and of the absorption band are shown in Fig. 8c for the same moment. The Murmansk ionosonde registered a particle E-layer at 22.15 plus simultaneously a- and r-types of sporadic ionization (E_s-layers at 22.30 UT (01.30 MLT). The electron density values derived from $f_B E_s$ were 5.0×10^{10} and 4.9×10^{11} m^{-3}, respectively. Both ionosonde measurement regions are located equatorward of the visual arc. The backscatter intensity distribution along the radar arc was similar to both previous events.

The specific peculiarity of this last event is the extreme quiescence of the ionosphere before the moment of the substorm onset. Indeed, B_z was positive for more than 1 h. The auroral absorption, sporadic ionization and ionospheric currents were practically absent for almost 10 h. Thus, the value of the background electric field was probably small and below threshold around the auroral arc. As in the previous examples, the electron density maximum (outside the arc) and the backscatter signal intensity maximum were registered at opposite sides of the visual arc. Besides, the electron density equatorward of the auroral arc was equal to or much higher than the ionization threshold for the appearance of a radar aurora. Therefore, the electric field was below threshold everywhere except in the region within the radar arc itself. As in the previous events, the signs of the H-component variations accompanying the increase in the backscatter intensity show that the total ionospheric electric field (convection plus arc-associated) as well as the large-scale convection electric field were predominantly southward.

The southward arc-associated electric field increases the density of the ionospheric current. Thus, in the morning, the radar arc manifests itself as a westward Hall-current enhancement flowing along the poleward edge of the auroral arc.

The histogram of the *minimum* distances between the radar and visual arcs along the meridian in the morning sector is shown in Fig. 9. It was constructed from the data of ten events where the auroral arcs were constantly observed in the zenith of the ASC (KEV, IVA, MUO and LPY), as mentioned in the previous section. The values of the distances, presented in Table 2, range from about 5 km to about 50 km. The mean value is about 25 km, and the median about 15 km.

Table 2. List of morning radar arcs with well-defined properties

Date	Year	UT	MLT	ASC	Distance	Width
October 20	1975	22.27	01.30	MUO	15±10	50
March 2	1976	21.34	00.30	KEV	8± 5	25
March 2	1976	21.57	01.00	IVA	40± 5	45
March 15	1978	20.25	23.30	LPY	20± 5	55
March 15	1978	21.24	00.30	KEV	50± 5	100
March 18	1978	00.55	04.00	KEV	5± 5	45
November 26	1978	00.06	03.00	IVA	45± 5	40
January 25	1979	02.11	05.15	IVA	10± 5	30
January 27	1979	23.36	02.30	MUO	25± 5	50
March 5	1979	02.18	05.15	KEV	5± 5	70

The near-midnight sector

The events studied here are observed after the convection reversal, which in our case takes place at about 18 UT, and before local magnetic midnight within the westward electrojet region. The short lifetime of the auroral arcs and their dynamical development is a characteristic feature of this sector. The time scale is an order of magnitude less than the corresponding times in the evening or morning sectors, 1–3 min only. It may be expected on general grounds that in this sector there are analogues of both the evening- and morning-type situations near the auroral arcs under different physical conditions. If the radar arc is located equatorward (poleward) of the visual arc, it should be of the evening (morning) type. Later on, we shall show that the physical conditions which prevail in either type of cases are rather different. For instance, the evening type is associated with the preceding recovery of the H-component variation almost up to its undisturbed level. The morning type is, on the contrary, associated with a sharp increase of the value of the negative H-component variation registered by ground-based magnetometers situated under the auroral arc considered.

Event 1. February 18, 1979. The locations of the radar and visual arcs at 20.27 UT (23.30 MLT), when the visual arc suddenly brightened considerably, are shown in Fig. 10a. The breakup started right after this moment. The meridional profiles of the H- and Z-component variations during the growth phase and just before the breakup are shown in Fig. 10b and Fig. 10c; also, the meridional locations of the visual and radar arcs are shown. It is seen that the westward electrojet intensity increased suddenly near the breakup moment in the region poleward of the visual arc. According to the riometer chain and ASC network data (not presented here), the main high-energy particle precipitation area was situated equatorward of the visual arc (Sergeev et al., 1983). Therefore, the strengthening of the westward electrojet intensity observed at 20.27 UT might be associated with the increase in the value of the southward component of the ionospheric electric field within the region poleward of the visual arc. According to the ASC data, no auroral bulge was formed at that moment, but rather 2 or 3 min later. It seems reasonable to associate the electric field value increase in the vicinity of the auroral arc with an additional contribution of the arc-associated electric field, which strengthened during the brightening of the arc. If the latter had a southward meridional component having a maximum at the poleward side of the arc, the resulting

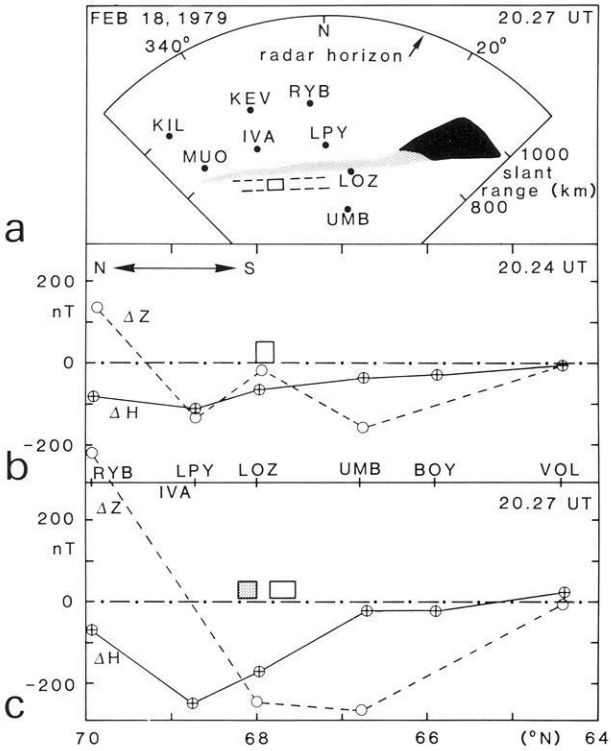

Fig. 10a–c. **a** The relative locations of the radar arc (*broad band*) and visual arc (*dashed lines*). The intensity level of the radar arc is shown by the degree of darkening in the band. **b, c** *Open rectangles* show the location of the visual arc as seen by the Ivalo ASC. The *dotted rectangle* shows the meridional location of the radar arc

electric field could become large enough to exceed the threshold for the appearance of a radar aurora in the region near the visual arc (and within the radar arc).

Event 2. November 24, 1978. Several examples of evening and morning types, based mainly on the Loparskaya ASC data and the Loparskaya H-component magnetometer record, are shown in Fig. 11. In the first example, the auroral arc at the southern edge of the auroral bulge brightened suddenly at 17.59 UT at the same time as the H-component recovered almost to its undisturbed level. The visual arc was accompanied by a radar arc of the evening type. Similar behaviour could be observed at 19.24 UT and 21.26 UT (00.10 MLT). The relative locations of the radar and visual arcs for the last moment are shown to the right in the figure, which was constructed from the Ivalo ASC film. The corresponding radar arc is of the evening type. The first example of the morning-type situation is illustrated in the figure at 18.14 UT. From the Loparskaya ASC film it is seen that this auroral arc was situated at the northern edge of the auroral bulge. In all similar situations, marked by downward arrows, sudden increases in the westward electrojet intensity were registered by the magnetometers nearest to the arc.

We have collected data from 19 events in the near-midnight sector in Table 3. In Fig. 12, we present the ΔH variations for these events. The distribution of ΔH variations shows consistently almost zero values for the evening type (dots) and large negative values for the morning type (crosses.

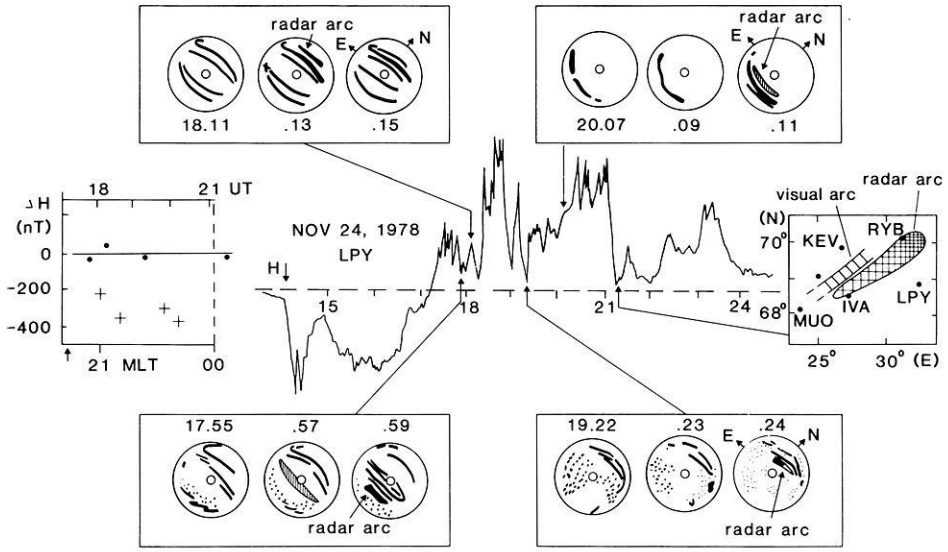

Fig. 11. Loparskaya ASC films (*top and bottom rectangles*) and the observatory magnetometer record showing the differences of the morning (*downward arrows*) and evening types (*upward arrows*). The map of the relative locations of the radar and visual arcs is constructed from the Essoyla radar and Ivalo ASC data. The distribution of the ΔH variations as registered by the ground-based magnetometer located under the arc is shown near the *left margin*. The evening-type events are denoted by *points*, and the morning types by *crosses*

Table 3. Near-midnight events

Date	Year	UT	MLT	ASC	ΔH	Magnetometer	Type
November 24	1978	17.59	20.45	LPY	− 43	LOZ	evening
November 24	1978	18.25	21.10	LPY	+ 10	LOZ	evening
November 24	1978	19.24	22.10	LPY	− 17	LPY	evening
November 24	1978	21.26	00.10	IVA	− 34	LPY	evening
March 3	1976	17.34	20.35	LPY	− 30	LOZ	evening
March 15	1978	19.08	23.10	KEV	0	RYB	evening
November 25	1978	18.11	20.55	IVA	−260	RYB	morning
November 24	1978	18.14	21.00	LPY	−220	RYB	morning
March 2	1976	19.50	22.50	IVA	−140	LPY	morning
November 24	1978	20.10	22.55	LPY	−330	RYB	morning
November 24	1978	20.20	23.05	LPY	−350	UMB	morning
February 27	1976	20.10	23.10	MUO	−165	LPY	morning
March 2	1976	20.10	23.10	MUO, KEV	−200	LPY	morning
February 18	1979	20.28	23.30	IVA	−175	LOZ	morning
March 15	1978	20.25	23.30	LPY	−110	LPY	morning
March 15	1978	21.24	00.25	KEV	−145	RYB	morning
March 15	1978	21.27	00.30	KEV	−190	RYB	morning
April 19	1982	22.07	01.07	LPY	−246	LPY	morning
September 8	1982	22.35	01.35	LPY	− 22	LPY	evening

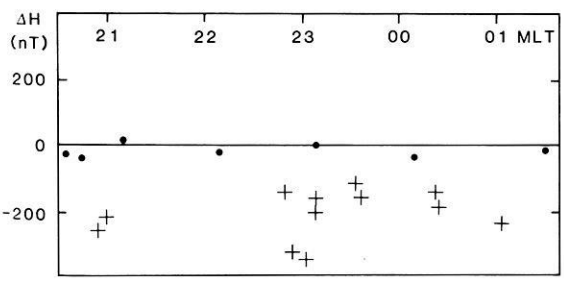

Fig. 12. The distribution of the ΔH variations registered by the ground-based magnetometer located under the arc for the 19 near-midnight events. *Points* mark the evening-type events, *crosses* the morning types

Event 3. March 6, 1979 is an example of a direct measurement in this MLT sector in the vicinity of an auroral arc (from Petrov et al., 1984) during the SAMBO campaign. The meridional component of the ionospheric electric field turned from south to north within the region equatorward of the westward-travelling auroral bulge. The balloon electrometer data gave a value of about 5 mV/m for the northward component. The evening radar arc appeared and lasted for 2 min in the region equatorward of the most southward auroral arc near the moment of the surge passage. This was observed at 20.58 UT, i.e. practically at local magnetic midnight. The small, near-zero meridional component of the ambient ionospheric electric field in the vicinity of an auroral arc was observed at the southern edge of the auroral bulge.

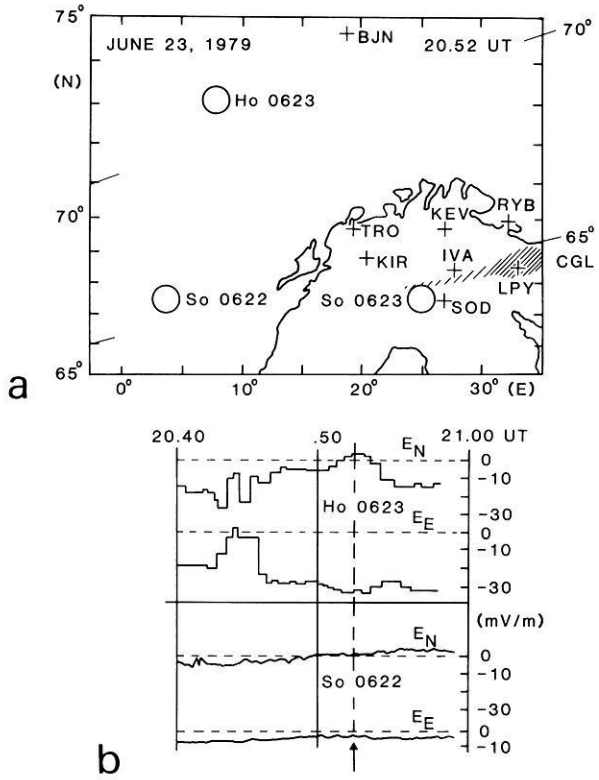

Fig. 13. The balloon positions relative to the radar arc at the moment of its appearance (*upper panel*). Geographic and corrected geomagnetic latitudes are given on the *left- and right-hand sides*, respectively. The *lower panel* contains the ionospheric electric field as measured by the balloons near the moment of interest, denoted by the *arrow*. The third balloon, So0623, could only register auroral precipitation

Event 4. June 23, 1979. In this case, the direct measurements of electric fields and particle precipitations were obtained simultaneously on three balloon flights close to magnetic midnight during a SBARMO experiment (Tanskanen et al., 1982). Figure 13 shows the positions of the radar arc and the electric field data. The radar arc appeared in a quiescent ionosphere at 00.05 MLT. According to the Kola magnetometer-chain data, the radar arc was observed within the westward electrojet region with an intensity of about 150 nT. The four riometers in Kevo, Ivalo, Sodankylä and Loparskaya detected the auroral absorption band during the whole growth phase interval, from 20.30 to the breakup at 21.02 UT. The band was located approximately at the equatorial edge of the radar arc appearing at 20.51 UT. The orientation of both forms was practically the same. As shown in the two previous sections, this is typical of the evening type of forms only. The marked eastward thickening of the radar arc also means that it was of the evening type. As already mentioned in the Introduction and shown for individual events (Tsunoda et al., 1976; Timofeev et al., 1980), such radar arcs are located close to and equatorward of the visual arcs. In this case, the visual arc could not be detected in midsummer. The lower panel of the figure shows that the ionospheric electric field components were directed westward and southward during the growth phase before the appearance of the radar arc. As in the previous event, the meridional component of the field passed through zero and remained northward for a few minutes near the moment of the radar arc appearance according to the data of both northern balloons. The great similarity of the electric-field variations registered on the two rather remote balloons shows that the spatial scale of variations is large. The third, southernmost balloon measured the intensity of auroral fluxes in several energy channels. According to these and the riometer chain data, no increase in the fluxes could be detected near the moment of the radar arc appearance. The Murmansk ionosonde data showed that the ionization density was well above the threshold for the radar aurora appearance both equatorward (at 20.45 UT) and poleward (at 21.00 UT) of the arc. The zonal component of the electric field surrounding the radar arc was constantly westward in accordance with the equatorward drift of the auroral forms.

Since the radar arc appeared in spite of the smallness of the background electric field, we have to conclude that a northward electric field with a value of about 15–20 mV/m is associated with the auroral arc on the southern edge of the bulge. We have no direct data on electric fields for the opposite side of the bulge, but inferring from the existence of the radar aurora in this region, we see that a southward electric field with a maximum poleward of the arc was associated with the auroral arc. The existence of such arc-associated electric fields has been proven for the event on February 18, 1979 (Fig. 10) for the active auroral arc situated within the region of southward ambient electric field. In our opinion, it is the ambient electric field which is the physical reason determining the differences in the orientation and location of the maximum of the arc electric field at the opposite edges of the bulge. The essential difference of these features is, in turn, reflected in the non-symmetrical behaviour of the ΔH variations discussed above.

Discussion

Introduction

Previous papers have usually described single examples of direct measurements of the parameters near an auroral arc (Casserly and Cloutier, 1975; Cloutier and Anderson, 1975; Cahill et al., 1978; Stiles et al., 1980; Robinson et al., 1981; for a list of references, see Marklund, 1984). Attempts to construct a classification scheme of the electric field patterns in the vicinity of an auroral arc were first made during the past few years (de la Beaujardière et al., 1981; Yasuhara, 1981; Baumjohann, 1983; Marklund, 1984).

De la Beaujardière et al. (1981) constructed a morphological scheme; their data set was practically empty of after-midnight sector events. Also, the account of the east-west electric-field components was very crude, the accuracy being of the order of 100% according to Marklund (1984). Yasuhara (1981) has applied the same morphological approach to rocket measurements. Baumjohann's review (1983) noted the remarkable difference in the spatial scales of the arc-associated electric field patterns registered by rockets (about 10 km) and by means of incoherent scatter facilities (up to about 100 km), but it was based on a few events only. The evening-to-morning asymmetry of the electric field patterns was shown in one case by comparing the data from two rocket flights. Marklund's scheme has a clear physical foundation at ionospheric level, and it distinguishes two physically different types of auroral arcs: polarization arcs and Birkeland current arcs. These types

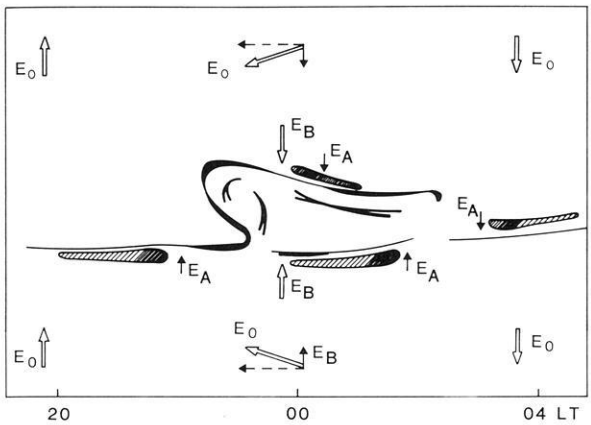

Fig. 14. A schematic representation of the relative locations of radar and visual arcs for different MLT values. Radar arcs are denoted by the *shading*, visual arcs by the *solid lines*. The arc-associated electric field must be above the level of RA appearance (15–30 mV/m). The letters *O*, *B* and *A* refer to convection, auroral bulge and auroral arc, respectively

differ in their mechanisms to satisfy the current continuity requirements across the arc. The distinction is made by comparing the electric fields and conductivities away from the arc (ambient parameters) and within the visual arc limits. Conclusions about the behaviour of electric fields in the intermediate region are not possible without additional assumptions. Alternatively, electric field pattern measurements in the vicinity of the auroral arc are necessary.

General

In this paper we have been able to draw conclusions about the electric field patterns in the vicinity of an auroral arc in different MLT sectors and under different ionospheric conditions on the basis of radar aurora data. In this sense, the method itself is a further development of Tsunoda et al. (1976), where the authors considered the sudden appearance of the radar arc during the visual arc brightening as being due to the increase in the electric field value in a previously quiescent ionosphere. The results obtained here are in agreement with their results in the evening sector, in spite of the large difference in the radar frequencies, 398 and 88 MHz. We have also been able to determine the minimum meridional distances between the visual and radar arcs.

It should be stressed that our data selection criterion, the presence of a radar arc in the close vicinity of an auroral arc, induces a bias. In fact, in such a way only brightening or bright auroral arcs are selected (Tsunoda et al., 1976; Timofeev and Yahnin, 1982). It probably means that we have selected the rather general asymmetrical type of the arc-associated electric field patterns (de la Beaujardière et al., 1981).

The electric field patterns

We do not claim that some of our results about the electric field patterns in the evening and morning sectors are particularly new; the same cannot be said about the near-midnight sector.

The results described in the previous sections are summarized in Fig. 14, where the spatial interrelations of the radar and visual arcs are shown. The meridional scale of the arc-associated electric field, the width of the radar arc, is about 100 km at ionospheric level for all MLT values. The orientation of the field in the evening and morning sectors is similar to that of the convection electric field. The regions of the electric field maxima are shifted equatorward or poleward of the visual arc in the evening- or morning-type situations, respectively. Near midnight, the characteristics of the electric field depend on which side of the auroral bulge the visual arc is situated.

For the evening sector, the arc-associated electric field patterns presented in Fig. 14 are in good agreement with the direct measurements quoted in the Introduction and with, for example, the review of Baumjohann (1983). Summarizing, the typical features of the evening radar arcs found in the previous section were:

1) The evening radar arc appears near the corresponding visual arc, always on its equatorward side. The arcs have practically the same spatial orientation and temporal development.

2) In the case of several discrete homogeneous auroral arcs, only the most southward arcs near the boundary dividing the eastward and westward electrojet regions, i.e. the convection reversal boundary, are accompanied by a radar arc.

3) The average meridional radar arc width is about 1° in latitude. The *minimum* meridional distance between the visual and radar arc is consistent with zero, i.e. of the order of the measurement accuracy, about 5 km.

4) The radar arcs are located within the eastward electrojet, where the electric field is northward. Sometimes during growth-phase conditions, the radar arcs are situated near the auroral absorption maximum.

In the evening sector, practically the same value of the meridional scale of the arc-associated electric field at ionospheric level has been measured by an incoherent scatter radar (Vondrak, 1981). In the morning sector, our results agree with the few known examples (Horwitz et al., 1978; Ziesolleck et al., 1983; Brüning et al., 1985). Summarizing, the typical features of the morning radar arcs were:

1) The morning radar arcs appear at the poleward side of the visual arc at a distance of about 10–20 km, and have the same orientation and development as the visual arc.

2) The morning radar arcs appear, or their intensity increases suddenly, at the same time as the westward electrojet intensifies (registered by ground-based magnetometers) or the visual arcs start brightening.

3) The radar arcs and the auroral absorption bands are located on opposite sides of the visual arcs, the radar arc being poleward and the absorption band equatorward of the visual arc. The relative distance between these two forms is about 100 km.

4) In most cases, the backscatter intensity maximum is located at the western edge of the radar arc in spite of the differences in aspect angle and flow angle conditions. The meridional width of the radar arc remains constant along the arc within the limits of the radar field of view. Frequently, the backscatter intensity distribution along the radar arc agress qualitatively with the luminosity distribution of the visual arc.

A point to be noted is the systematical difference in the radar diagnostic features between the evening and morning sectors. In the morning sector, the smallness of the flow angle dependence of the radar echo with respect

to the evening radar arc auroral echo may not be connected with any systematical difference of the electric field patterns in these MLT sectors. The difference in the flow angle dependences between the morning and evening hours was also noted by André (1983). Timofeev (1985) made a systematical study and suggested that this phenomenon is a result of the inner granular structure of the diffuse backscatter in the morning sector reported by Greenwald (1979) and Vasilyev (1981), and concluded that the morning radar arc is a narrow meridional band of the normal diffuse granular morning backscatter, in the same way as the evening radar arc is a narrow meridional band of the usual evening diffuse backscatter (Tsunoda et al., 1976). This would then mean that all nightside auroral oval radar arcs are narrow meridional bands of diffuse backscatter generated mainly by the enhancement in the level of the ionospheric electric fields in the vicinity of the auroral arc. The difference may also be due to the difference in the spatial forms of the auroral irregularities when looked at by a radar parallel or antiparallel to the current flow direction in the eastward or westward electrojet regions (Sverdlov, 1986; Sverdlov et al., 1986).

Summarizing, the typical situation in the vicinity of an auroral arc in the midnight sector was found to be the following:

1) The type is determined by the location of the auroral arc relative to the auroral bulge and/or the sign of the ΔH variation under the arc.

2) The morning-type situation, with the radar arc located poleward of the visual arc, occurs at the poleward edge of the auroral bulge and is associated with rather large negative values of the ΔH variations, about -200 nT.

3) The evening-type situation, with the radar arc located equatorward of the visual arc, occurs at the equatorward edge of the auroral bulge and is associated with the H-component recovery up to its undisturbed level. The average values of the corresponding ΔH variations are about -20 nT and the value of the meridional component of the ambient electric field is small and positive, about $+5$ mV/m. An electric field of 10–25 mV/m is associated with the visual arc near the southern edge of the bulge.

Isaev et al. (1985) give a direct test of the above ground-based results by comparing simultaneous particle and electric field measurements on board the IK-BULGARIA-1300 satellite. The radar arc was observed poleward of the visual arc, as expected in the morning-type case. The southward component of the measured electric field had a maximum poleward of the visual arc. The particle flux corresponding to diffuse auroral luminosity had a maximum equatorward of the visual arc.

The conductivity profiles, ionospheric and field-aligned currents

The aim of the present paper is to construct a scheme of the full three-dimensional current system associated with the visual and radar arcs. As we have seen earlier, the radar arc can be considered as a Hall-current enhancement; already Baumjohann et al. (1978) have noted that the maximum of the backscatter intensity coincided with the region of the Hall-current maximum. The field-aligned currents in the vicinity of an auroral arc may be obtained from the divergence of the horizontal height-integrated ionospheric currents. There, we need to know the electron density or conductivity profiles. Since we are interested in the general three-dimensional patterns of the currents, the average E-layer ionization profiles are sufficient. For a rough modelling of the profiles, we use optical and riometer data.

In our estimates of the FAC directions we use three different conductivity (electron density) profiles:

– the asymmetric triangle model (Fig. 15a, d) based on very accurate scanning photometer data (Velichko et al., 1981) with uniquely large statistics of brightening auroral arc measurements (about 100 events from nearly 10 years of observations)

– the constant conductivity model (Fig. 15b, e) based on incoherent scatter radar data (de la Beaujardière et al., 1977; Stiles et al., 1980; de la Beaujardière et al., 1981)

– the gap-like conductivity model (Fig. 15c) (Lui et al., 1977; Robinson et al., 1981; Marklund et al., 1982) for the evening type.

The results of the qualitative analysis on the basis of these three profiles are presented in Fig. 15. As one can see, the auroral-arc–radar-arc system is part of a Birkeland current sheet loop. The downward FACs are located equatorward of the visual arc in the evening and poleward in the morning, and the upward FACs. Similar FAC configurations near the arc have been found by direct measurements (Casserley and Cloutier, 1975; Robinson et al., 1981; de la Beaujardière and Vondrak, 1982; Theile and Wilhelm, 1980). In these experiments, the spatial scales along the meridian vary from a few tens to about one hundred kilometres. This range of values is in good agreement with the average meridional width of the radar arc or the arc-associated electric field obtained in this paper (Table 2).

It follows from our scheme that the region of upward FACs is wider than the visual arc and that additional small-scale FAC loops (denoted by dashed lines in Fig. 15) appear in some situations. These features are sometimes detected in rocket experiments (Robinson et al., 1981; Marklund et al., 1982; Ziesolleck et al., 1983). The current flow directions in the small-scale loops, either deduced from direct measurements or derived from the divergence of the ionospheric horizontal currents, are the same: counterclockwise in the evening (Robinson et al., 1981; Marklund et al., 1982) and clockwise in the morning (Ziesolleck et al., 1983). These findings support the view that the asymmetric type of the arc-associated electric field is rather general, and practically all known experimental features of the three-dimensional current systems associated with an auroral arc can be explained.

It must be noted that the conclusion about the loop character of the three-dimensional currents associated with the visual-arc–auroral-arc system depends to a certain degree on the ratio of the characteristic scales of both the electron density and electric field profiles used. The same conclusion may be supported by an independent argument. As noted earlier in this section, the radar arc may be considered as a band of zonal Hall current enhancements. Since the ratio of Hall and Pedersen conductivities, Σ_H/Σ_P, is constant outside the visual arc, the meridional current is stronger within the radar arc limits. Since there is an upward FAC within the visual arc, we may conclude from current conservation that there is also a downward FAC within (or near) the radar arc limits, which shows the existence of a Birkeland current loop with a meridional scale of about the size of the system, i.e. a few tens of kilometres.

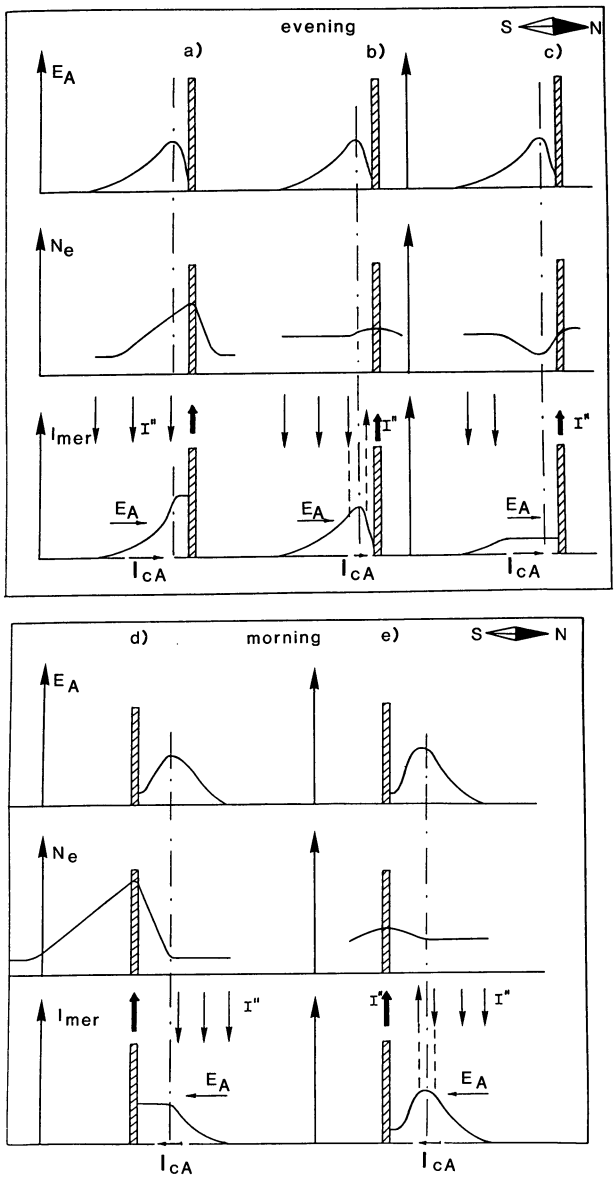

Fig. 15a–e. Sketch of near-arc electric field and three-dimensional current patterns for various types of conductivity profiles. *Shaded vertical strips* denote the visual arcs. The *top figures* show the arc-associated electric fields E_A, the *middle ones* the electron density profiles and the *bottom figures* the meridional current profiles. The field-aligned currents are denoted by I'' and shown by the *thick arrows*, the arc-associated closing currents by I'_{cA} and denoted by the *smaller horizontal arrows*. Also, additional small field-aligned current loops denoted by *dashed lines* are shown

The auroral bulge

The scheme proposed here may be stated: away from midnight, the direction of the arc-associated electric field in the radar arc region is the same as that of the large-scale convection electric field, i.e. northward in the evening, southward in the morning. In general, and especially near midnight, this must be phrased as follows: the meridional ionospheric closing currents of the three-dimensional current systems of the auroral-arc–radar-arc system and of the large-scale convection field are approximately parallel.

We choose the x-axis towards the magnetic north and the y-axis eastward. Then the meridional component I_x of the closing current of the convection field near midnight is determined by both the meridional and zonal components of the convection electric field (E_x and E_y) by the usual Ohm's law:

$$I_x = \Sigma_P E_x - \Sigma_H E_y, \tag{1}$$

where the Σ_P and Σ_H are the height-integrated Pedersen and Hall conductivities.

Near the southern edge of the auroral bulge, the meridional component of the convection electric field is approximately zero. This is due to the compensation of the small southward convection electric field by the electric field associated with the bulge (see Fig. 14). The bulge has its own electric field created by the negative charge located within the head of the bulge (Inhester et al., 1981; Opgenoorth et al., 1983; Petrov et al., 1984). The compensation is demonstrated, e.g., in Tanskanen et al. (1982); Petrov et al. (1984), and may be confirmed by a comparison of the statistics on ground-based magnetic variations and ionospheric electric fields (Kamide and Vickrey, 1983). According to these data, the average value of the H-component variations obtained here for the southern edge of the bulge corresponds to a value of the meridional component of the total ionospheric electric field of not more than ± 5 mV/m.

The zonal component of the electric field at the southern edge of the auroral bulge is systematically observed to be westward near midnight (Mozer and Lucht, 1974; Zi and Nielsen, 1981; Baumjohann et al., 1981). Hence, according to Eq. (1), the meridional convection current is northward, since the meridional electric field is almost zero and the zonal component is westward: $I_x > 0$, since $E_x \approx 0$ and $E_y < 0$. In the model proposed here (see Fig. 15), the meridional current of the Birkeland current loop of an auroral arc is also northward in this region.

The reverse happens when one goes to the opposite edge of the auroral bulge. There, the bulge-associated field and the convection electric field add up. Inferring from the sign and the average value of the H-component variations (-200 nT) on the ground, the total southward electric field provides the large values of the westward and southward ionospheric currents in this region. In the model proposed here (see Fig. 15), the meridional current associated with an auroral arc is likewise southward.

If the H-component variations are considerably smaller than the average value -200 nT, the value of the total ionospheric convection current is probably nearly zero. The absence of radar arcs in similar situations shows that the currents and electric fields associated with such auroral arcs are also small. Then an enhancement in the circuit, in the value of the meridional closing current, is possible if the westward component becomes unusually large. This happens in the data on March 21, 1973 [see Fig. 5c, d and Fig. 2 in Tsunoda et al. (1976)]: at about 07.20 UT an evening-type situation was encountered. The radar arc was detected on the equatorward side of the most southward arc, the H-component variation was about -100 nT, and the ionospheric electric field was westward and had an unusually large value of 40 mV/m.

The current systems

We have seen that the meridional closing currents of the Birkeland current loops associated with an individual auroral arc and those of the large-scale convection currents are

analogous, i.e. the three-dimensional current system associated with an auroral arc is similar to the current circuit associated with the large-scale convection in the whole nightside auroral oval.

Also, control of the direction of the inverted-V-associated electric fields by the convection electric field surrounding the structure has been described in Heelis et al. (1981). The similarity in the behaviour of the two electrodynamical systems, the auroral arc and the inverted-V, with respect to the convection electric field patterns is striking. We may speculate that the direction of the current flows of the three-dimensional current systems coupling the ionosphere and the magnetosphere does not depend on the spatial scale of the structure, but only on the character of the convection flow around the structure (Kaufmann, 1984). In other words, as electrodynamical systems, both the auroral arcs and the inverted-V events are cells of enhanced convection having only different spatial scales, 10 and 100 km at ionospheric level, respectively. Recent AUREOL-3 satellite observations together with radar data support this view (Timofeev et al., 1985a). Also, it has been noted by Fennel et al. (1981) that the visual arcs have a tendency to be observed at the edges of the inverted-V structures.

The electron density depression

As noted in Baumjohann (1983), the region of the maximum of the arc-associated electric field is located farther away from the visual arc in the morning (Ziesolleck et al., 1983) than in the evening (Marklund et al., 1982). Our data shows that this is indeed so, systematically: the minimum distance between the visual arc and the region of the arc-associated electric field enhancement, the radar arc, is on average about 15 km in the morning and consistent with zero (with an accuracy of 5 km) in the evening. The reason for this systematic difference is, in our opinion, connected with the gap-like character of the conductivity profile often observed in the evening auroral arc (Robinson et al., 1981; Marklund et al., 1982). The electron density depression (gap) is located equatorward of the auroral arc, which is within the limits of the arc-associated Birkeland current loop in the evening, but outside in the morning. Therefore, its influence on the current system must be taken into account in the evening sector only. The meridional size of this gap is, according to the direct measurements quoted, 10–20 km, which is about one-tenth of the meridional scale of the arc-associated Birkeland current loop. By current conservation, the arc-associated electric field within the density depression region should increase, and the electric field maximum should therefore be located in general closer to the visual arc than in the gapless case. A rough estimate of this shift is half the size of the gap in the ionosphere, i.e. 5–10 km, which is not too far from the observed median (or average) based on much larger statistics.

Comparison with other models

It is well known that the auroral arc results from the ionosphere-magnetosphere coupling (Atkinson, 1970; Sato and Holzer, 1973; Maltsev et al., 1977; Mallincrodt and Carlson, 1978; Sato, 1978; Tverskoi, 1982). Leontyev and Lyatsky (1982) give a detailed description of the effects of ambient ionospheric electric field on the auroral arc electrodynamics. Their model is in complete agreement with the three-dimensional current system picture developed in this paper. However, it only describes the visual part of the auroral arc system. Thus, the meridional size of the arc current loop system in this model is only about 10 km at ionospheric level. The Sato (1978) model gives it approximately the same size as the present model, and the three-dimensional current system constructed is also in full agreement with the systematics of this paper for the whole nightside auroral oval. Recently, Sato's idea that the electrodynamical system of the auroral arc is a cell of enhanced magnetospheric convection in the ionosphere-magnetosphere coupling has been developed further by Trakhtengertz and Feldstein (1984).

The model presented here is based on the idea that a close connection exists between the convection electric field pattern and the auroral arc electrodynamical system. The model predicts the existence of an arc-associated electric field beyond the limits of the visual arc. The location of the maximum of the electric field is predicted to shift to a distance of about 10 km towards the region of inflow of the downward FAC current of the auroral arc current loop. This value is in rough agreement with the data presented here. Moreover, the model can in principle explain the systematic difference in the location of the arc-associated electric field maximum relative to the visual arc between the morning and evening types of radar arcs. This difference is, in the model, due to the electron density depression in the vicinity of the evening arc. The model proposed by Vondrak (1975) is in agreement with the data far from midnight only. Near the midnight meridian, when the westward component of the electric field dominates, Vondrak's model is in disagreement with our data.

Joule heating

According to our model (see Figs. 14 and 15), the work per unit area done by the arc-associated electric forces,

$$W_A = E_A \cdot I_A \tag{2}$$

where E_A and I_A are the arc-associated electric field and current, respectively (see Figs. 14 and 15), is positive in the vicinity of the arc and within the radar arc for all MLT values. In the evening sector, this agrees with incoherent scatter data (Stiles et al., 1980; Robinson et al., 1981; de la Beaujardière et al., 1981) showing the presence of an increased Joule heating area with a meridional size of about 100 km located equatorward of the visual arc near its equatorial edge. Accurate rocket measurements of ionospheric electric fields and conductivities during an auroral arc passage showed that the electric field meridional component sometimes decreased down to zero under the influence of the polarization electric field only (Marklund, 1984). In such a case, the arc polarization electric field within the visual arc and the arc-associated electric field within the radar arc may be estimated to be approximately equal. To the extent that the electric fields may be considered as uniform within the visual arc, the arc polarization electric field and the ionospheric closing current of the arc current circuit are antiparallel within the visual arc, meaning that the visual arc acts like a generator. On the other hand, within the radar arc the arc-associated electric field and the ionospheric closing current are parallel, which means that the radar arc acts like a load. Putting in characteristic values for the

meridional scales and Pedersen conductivities for the visual arc, 10 km and 10 S, versus the numbers for the radar arc, 100 km and 1 S, we see that the total energy release within the radar arc is at least one order of magnitude higher than the energy input from the visual arc. Therefore, it is important to recognize that the electric generator of the three-dimensional current system associated with the auroral arc is located outside the ionosphere, i.e. in the magnetosphere.

Conclusions

1) Discrete radar arcs of evening type are observed in the evening sector and near midnight at the southern edge of the auroral bulge; discrete radar arcs of morning type are observed in the morning and at the northern edge of the bulge. Radar arcs of evening type appear equatorward of the corresponding visual arcs, those of the morning type poleward. The radar and visual arcs have the same orientation and appear, brighten and move in harmony in all MLT sectors. The arcs are manifestations of a common underlying structure whose meridional size is about 1° in latitude, i.e. 100 km at ionospheric level for all MLT values.

2) The radar arc is a Hall current band enhancement caused by the presence of an arc-associated electric field within the band. For the whole nightside oval, there are two types of arc-associated electric field patterns corresponding to the two types of radar arcs. Far from midnight, the spatial orientation of the field and the orientation of the ionospheric convection electric field are the same: northward in the evening, southward in the morning.

3) The minimum meridional distance between the visual arc and the radar arc, the manifestation of the arc-associated electric field, is on average consistent with zero in the evening and about 15 km in the morning. This difference is probably due to differences in the meridional conductivity profiles through the arc in these MLT sectors, in particular to the existence of an electron density depression in the arc current circuit in the evening.

4) The construction of the three-dimensional current system associated with an auroral arc and a radar arc shows that the arc, as an electrodynamical system, is a Birkeland current sheet with an upward FAC within the visual arc and a downward FAC within the radar arc. The meridional size of the system is a few tens of kilometres at ionospheric level.

5) The direction of the meridional closing current of the arc Birkeland current loop is the same as that of the meridional ionospheric convection current in the vicinity of the visual arc. Around magnetic midnight, it is determined by both the meridional and zonal components of the convection electric field.

6) The work done by the electric forces in the arc Birkeland current loop is positive everywhere within the radar arc for the whole nightside auroral oval. The total amount of work done within the radar arc limits is probably at least an order of magnitude larger than the total energy input within the visual arc limits. Therefore, the generator of the arc current circuit is most probably located outside the ionosphere, i.e. in the magnetosphere.

7) From the similarity of the large-scale convection electric field patterns and those of the auroral arc, it follows that the auroral arc as an electrodynamical system is a cell in the large-scale convection structure. Recent coordinated satellite-ionosphere experiments show that the inverted-V-events behave similarly (Isaev et al., 1985; Timofeev et al., 1985a, 1985b). Therefore, the radar-arc – visual-arc – inverted-V structure is a common electrodynamical pattern in the magnetosphere-ionosphere system.

Acknowledgements. The authors are grateful to V.M. Tolychkin and E.P. Vasilyev for the careful and continuous operating of the Essoyla radar and of the Kola magnetic chain. We thank Drs. W. Baumjohann, G. Marklund, Yu.P. Maltsev, S.V. Leontyev, V.A. Sergeev, M.I. Pudovkin, Yu.I. Galperin and V.B. Lyatsky for fruitful discussions and remarks, as well as Dr. O.M. Raspopov for his help and concern and Dr. M. Uspensky for constructive criticism. We also thank Mrs. N.I. Lomakina and T.I. Roldugina for help in preparing the manuscript. This work has been supported financially by the Finnish-Soviet Committee on co-operation in science and technology and the Finnish Academy.

References

Akasofu, S.-I.: Auroral arcs and auroral potential structure. In: Physics of auroral arc formation, Akasofu, S.-I. and Kan, J.R., eds.: pp. 1–14. Washington, D.C.: A.G.U. 1981

André, D.: On the dependence of the relative backscatter cross section of 1-m density fluctuations in the auroral electrojet on the angle between electron drift and radar wave vector. J. Geophys. Res. **88**, 8043–8050, 1983

Atkinson, G.: Auroral arcs: results on interaction of a dynamic magentosphere with the ionosphere. J. Geophys. Res. **75**, 4746–4756, 1970

Baumjohann, W.: Ionospheric and field-aligned current systems in the auroral zone: a concise review. Adv. Space Res. **2**, 55–62, 1983

Baumjohann, W., Greenwald, R.A., Küppers, F.: Joint magnetometer array and radar backscatter observations of auroral currents in Northern Scandinavia. J. Geophys. **44**, 373–383, 1978

Baumjohann, W., Pellinen, R.J., Opgenoorth, H.J., Nielsen, E.: Joint two-dimensional observations of ground magnetic and ionospheric electric fields associated with auroral zone currents: current systems associated with local auroral breakups. Planet. Space Sci. **29**, 431–447, 1981

de la Beaujardière, O., Vondrak, R.: Chatanika radar observations of the electrostatic potential distribution of an auroral arc. J. Geophys. Res. **87**, 797–809, 1982

de la Beaujardière, O., Vondrak, R., Baron, M.: Radar observations of electric fields and currents associated with auroral arcs. J. Geophys. Res. **82**, 5051–5062, 1977

de la Beaujardière, O., Vondrak, R., Heelis, R., Hanson, W., Hoffman, R.: Auroral arc electrodynamic parameters measured by AE-C and the Chatanika radar. J. Geophys. Res. **86**, 4671–4685, 1981

Brüning, K., Goertz, C.K., Wilhelm, K.: Why does the perpendicular electric field increase at the edge of auroral arcs? Adv. Space Res. **5**, 79–82, 1985

Burke, W.J., Hardy, D.A., Rieh, F.J., Kelley, M.C., Smiddy, M., Shuman, B., Sagalyn, R.C., Vancour, R.P., Widman, J.L., Lai, S.T.: Electrodynamic structure of the late evening sector of the auroral zone. J. Geophys. Res. **85**, 1179–1193, 1980

Cahill, L.J., Jr., Greenwald, R.A., Nielsen, E.: Auroral radar and rocket double-probe observations of the electric field across the Harang discontinuity. Geophys. Res. Lett. **5**, 687–690, 1978

Casserly, R.T., Jr., Cloutier, P.A.: Rocket-based magnetic observations of auroral Birkeland currents in association with structured auroral arc. J. Geophys. Res. **80**, 2165–2168, 1975

Chesnut, W.G.: Low frequency waves and irregularities in the auroral ionosphere as determined by radar measurements. In: Low frequency waves and irregularities in the ionosphere, N. D'Angelo, ed.: pp. 173–191. Dordrecht, Holland: D. Reidel 1968

Cloutier, P.A., Anderson, H.R.: Observation of Birkeland currents. Space Sci. Rev. **17**, 563–587, 1975

Fennel, J.F., Corney, D.J., Mizera, P.F.: Auroral particle distribution functions and their relationship to inverted Vs and auroral arcs. In: Physics of auroral arc formation, Akasofu, S.-I. and Kan, J.R., eds.: pp. 91–102. Washington, D.C.: A.G.U. 1981

Fremouw, E.J., Fang, D.J.: An all-sky camera format for radar auroral studies. Radio Sci. **10**, 891–904, 1975

Greenwald, R.A.: Studies of currents and electric fields in the auroral zone ionosphere using radar auroral backscatter. In: Dynamics of the magnetosphere, Akasofu, S.-I., ed.: pp. 213–248. Dordrecht, Holland: D. Reidel 1979

Greenwald, R.A., Weiss, W., Nielsen, E., Thomson, N.R.: STARE: a new radar auroral backscatter experiment in northern Scandinavia. Radio Sci. **13**, 1021–1039, 1978

Heelis, R.A., Hansen, W.B., Burch, J.L.: AE-C observations of electric fields around auroral arcs. In: Physics of auroral arc formation, Akasofu, S.-I. and Kan, J.R., eds.: pp. 154–163. Washington, D.C.: A.G.U. 1981

Horwitz, J.L., Doupnik, J.R., Banks, P.M.: Chatanika radar observations of auroral zone electric fields, conductivities and currents. J. Geophys. Res. **83**, 1463–1481, 1978

Inhester, B., Baumjohann, W., Greenwald, R.A., Nielsen, E.: Joint two-dimensional observations of ground magnetic and ionospheric electric fields associated with auroral zone currents. 3. Auroral zone currents during the passage of a westward travelling surge. J. Geophys. **49**, 155–162, 1981

Isaev, N.V., Yahnin, A.G., Bilichenko, S.V., Lazarev, V.I., Stanev, G., Teodosiev, D., Petkov, N., Timofeev, E.E., Trushkina, E., Chmyriev, Y.M.: A comparison of satellite measurements of electric and magnetic fields and particle fluxes with ground-based geophysical data. Adv. Space Res. **5**, 101–107, 1985

Kamide, Y., Vickrey, J.F.: Variability of the Harang discontinuity as observed by the Chatanika radar and the IMS Alaska magnetometer chain. Geophys. Res. Lett. **10**, 159–162, 1983

Kaufmann, R.L.: What auroral electron and ion beams tell us about magnetosphere-ionosphere coupling. Space Sci. Rev. **37**, 313–397, 1984

Leontyev, S.V., Lyatsky, W.B.: Solitary auroral arc generation. Planet. Space Sci. **30**, 1–4, 1982

Lui, A.T.Y., Venkatesan, D., Anger, C.D., Akasofu, S.-I., Heikkila, W.J., Winningham, J.D., Burrows, J.R.: Simultaneous observation of particle precipitations and auroral emissions by the ISIS-2 satellite in the 19–24 MLT sector. J. Geophys. Res. **82**, 2210–2226, 1977

Mallincrodt, A.J., Carlson, C.W.: Relations between transverse electric fields and field-aligned currents. J. Geophys. Res. **83**, 1426–1432, 1978

Maltsev, Yu.P., Lyatsky, W.B., Lyatskaya, A.M.: Currents over the auroral arc. Planet. Space Sci. **25**, 53–57, 1977

Marklund, G.: Auroral arc classification scheme based on the observed arc-associated electric field pattern. Planet. Space Sci. **32**, 193–211, 1984

Marklund, G., Sandahl, I., Opgenoorth, H.: A study of the dynamics of a discrete auroral arc. Planet. Space Sci. **30**, 179–197, 1982

Mozer, F.S., Lucht, P.: The average auroral zone electric field. J. Geophys. Res. **79**, 1001–1006, 1974

Nielsen, E., Greenwald, R.A.: Variations in ionospheric currents and electric fields in association with absorption spikes during the substorm expansion phase. J. Geophys. Res. **83**, 5645–5654, 1978

Opgenoorth, H.J., Pellinen, R.J., Baumjohann, W., Nielsen, E., Marklund, G., Eliasson, L.: Three-dimensional current flow and particle precipitation in a westward travelling surge (observed during the Barium-GEOS rocket experiment). J. Geophys.Res. **88**, 3138–3152, 1983

Pellinen, R.J.: IMS ground observations of optical aurora and ionospheric absorption made in Northern Europe with examples of data handling. In: The IMS source book, Russell, C.T. and Southwood, D.J., eds.: pp. 117–123. Washington D.C.: A.G.U. 1982

Petrov, V.G., Kozelova, T.V., Lazutin, L.L., Treilhou, J.-P.: Distribution of electric field near a westward travelling polar surge. Geomagn. Aeron. **24**, 194–197, 1984

Robinson, R.M., Bering, E.A., Vondrak, R.R., Anderson, H.R., Cloutier, P.A.: Simultaneous rocket and radar measurement of currents in an auroral arc. J. Gephys. Res. **86**, 7703–7717, 1981

Sato, T.: A theory of quiet auroral arcs. J. Geophys. Res. **83**, 1042–1048, 1978

Sato, T., Holzer, T.E.: Quiet auroral arcs and electrodynamic coupling between the ionosphere and the magnetosphere, 1. J. Geophys. Res. **78**, 7314–7329, 1973

Sergeev, V.A., Yahnin, A.G., Pellinen, R.J.: Relative arrangement and magnetospheric sources of zones of energetic electron injection, diffuse and discrete auroras during the preliminary phase of a substorm. Geomagn. Aeron. **23**, 792–796, 1983

Siren, J.C., Doupnik, J.R., Ecklund, W.L.: A comparison of auroral currents measured by the Chatanika radar with 50 MHz backscatter observed from Anchorage. J. Geophys. Res. **82**, 3577–3641, 1977

Starkov, G.V., Oksman, J., Uspensky, M.V., Kustov, A.V.: On the dependence of radar aurora amplitude on ionospheric electron density. J. Geophys. **52**, 49–52, 1983

Stiles, G.S., Foster, J.C., Doupnik, J.R.: Prolonged radar observations of an auroral arc. J. Geophys. Res. **85**, 1223–1234, 1980

Sverdlov, Yu.L.: A spatial–temporal approach to the Farley-Buneman instability. 1. Evolution of plasma irregularities in the crossed electric and magnetic fields (in Russian). Radiofizika. Izvestiya vuzov 1986 (in press)

Sverdlov, Yu.L., Miroshnikova, T.V., Sergeeva, N.G.: A spatial–temporal approach to the Farley-Buneman instability. 2. Effective cross section of the backscatter from auroral irregularities (in Russian). Radiofizika. Izvestiya vuzov 1986 (in press)

Tanskanen, P., Bjordal, J., Block, L.P., et al.: SBARMO-79: a multi-balloon campaign in the auroral zone. In: The IMS source book, Russell, C.T. and Southwood, D.J., eds.: pp. 153–158. Washington D.C.: A.G.U. 1982

Theile, B., Wilhelm, K.: Field-aligned currents above an auroral arc. Planet. Space Sci. **28**, 351–355, 1980

Timofeev, E.E.: About the systematical evening-to-morning differences of radiophysical characteristics of radar arcs. In: Aurorae (in Russian) **32**, pp. 89–94. Moscow 1985

Timofeev, E.E., Yahnin, A.G.: On the distribution of radio aurora types relative to the auroral bulge. In: Aurorae (in Russian), Isaev, N.G. and Starkov, G.V., eds.: **30**, pp. 32–43. Moscow 1982

Timofeev, E.E., Yahnin, A.G., Dmitriyeva, N.P.: Characteristics of radar arcs accompanying evening auroral arcs. Geomagn. Aeron. **20**, 535–538, 1980

Timofeev, E.E., Yahnin, A.G., Kozelova, T.V., Vasilyev, E.P., Vallinkoski, M.K., Pellinen, R.J.: Experimental study of arc-associated electric fields depending on physical conditions in the ionosphere, XVIII General Assembly IAGA, Bull. 48, Programme and Abstracts 1983

Timofeev, E.E., Smyshliaev, V.M., Jorjio, N.V., Galperin, Yu.I., Bosqued, J.M., Berthelier, J.J., Vallinkoski, M.K., Pellinen, R.J.: Coordinated data on auroral electrodynamics from ground-based radar diagnostics and AUREOL-3 satellite. In: Results of Arcad-3 project and of the recent programs in magnetospheric and ionospheric physics, pp. 949–971. Toulouse, France: CNES 1985a

Timofeev, E.E., Kozelova, T.V., Vallinkoski, M.K., Pellinen, R.J.: Auroral arc as an electrodynamical system. Review of the experiments. In: Proceedings of the first Soviet-Finnish auroral workshop, October 1–6, 1984, Pellinen, R.J. and Uspensky, M.V., eds: Sodankylä report series **44**, pp. 188–194, 1985b

Trakhtengertz, T.Yu., Feldstein, A.Ya.: Quiet auroral arcs: ionosphere effect of magnetospheric convection stratification. Planet. Space Sci. **32**, 127–134, 1984

Tsunoda, R.T., Presnell, R.I.: On the threshold electric field associated with the 398 MHz diffuse radar aurora. J. Geophys. Res. **81**, 88–96, 1976

Tsunoda, R.T., Presnell, R.I., Kamide, Y., Akasofu, S.-I.: Relationship of radar aurora, visual aurora and auroral electrojet in the evening sector. J. Geophys. Res. **81**, 6005–6015, 1976

Tverskoi, B.A.: Nature of homogeneous polar auroral arcs. Geomagn. Aeron. **22**, 794–799, 1982

Uspensky, M.V., Pellinen, R.J., Baumjohann, W., Starkov, G.V., Nielsen, E., Sofko, G., Kaila, K.U.: Spatial variations of ionospheric conductivity and radar auroral amplitude in the eastward electrojet region during pre-substorm conditions. J. Geophys. **52**, 40–48, 1983

Vasilyev, I.N.: Substorm in radar aurora. In: Irregularities in the ionosphere (in Russian), Shaftan, V.A., ed.: pp. 52–65. Yakutsk, USSR. Publ. of the Siberian Branch of USSR Acad. of Science 1981

Velichko, V.A., Samsonov, V.P., Nadubovich, Yu.A.: Vertical and horizontal profiles of the surface brightness of discrete auroral forms in 4278 and 6300 Å emissions. In: Aurorae and airglow (in Russian), Isaev, S.I., Nadubovich, Yu.A., Evlashin, L.S., eds.: **28**, pp. 35–40. Moscow 1981

Vondrak, R.R.: Model of Birkeland currents associated with an auroral arc. J. Geophys. Res. **80**, 4011–4014, 1975

Vondrak, R.R.: Chatanika radar measurements of the electrical properties of auroral arcs. In: Physics of auroral arc formation, Akasofu, S.-I. and Kan, J.R., eds.: pp. 185–191. Washington, D.C.: A.G.U. 1981

Yasuhara, F.: The perpendicular electric field associated with an auroral arc. Observations and their interpretations: A review. In: Magnetospheric dynamics, proceedings of the 1980 ISAS symposium on magneto-ionosphere. Kamide, Y., Nishida, A., eds.: pp. 34–42. Institute of Space and Aeronautical Science, Univ. of Tokyo 1981

Zi, M., Nielsen, E.: Spatial variations of ionosphere electric fields at high latitudes on magnetic quiet days. In: Exploration of the upper atmosphere. Deehr, C.S. and Holtet, J.A., eds.: pp. 293–304. Dordrecht, Holland: D. Reidel 1981

Ziesolleck, C.,Baumjohann, W., Brüning, K., Carlson, C.W., Bush, R.I.: Comparison of height-integrated current densities derived from ground-based magnetometer and rocket-borne observations during the Porcupine F3 and F4 flights. J. Geophys. Res. **88**, 8063–8072, 1983

Received February 11, 1986; revised version January 15, 1987
Accepted January 22, 1987